$G_{\alpha q}$ sensitizes TRPM8 to inhibition by $PI(4,5)P_2$ depletion upon receptor activation

Short title: Mechanism of receptor-induced inhibition of TRPM8

Luyu Liu, Yevgen Yudin, Chifei Kang#, Natalia Shirokova, Tibor Rohacs

Department of Pharmacology, Physiology and Neuroscience, Rutgers New Jersey Medical School, Newark NJ 07103

Corresponding author: Tibor Rohacs, tibor.rohacs@rutgers.edu, Department of Pharmacology, Physiology and Neuroscience, Rutgers New Jersey Medical School, 185 South Orange Ave, Newark NJ 07103

#current address: Department of Medicine, Division of Endocrinology, Icahn School of Medicine at Mount Sinai, New York, NY 10029

The authors declare no financial conflict of interest

ACKNOWLEDGEMENTS:
T.R. was supported by NIH grants NS055159 and GM093290. The authors thank Dr. Joshua Berlin for his insightful comments, Dr. David Julius (UCSF) for providing the TRPM8 clone, Dr. David McKemy (University of Southern California) for providing the GFP-TRPM8 mouse line, Dr. Yasushi Okamura (Osaka University, Japan) for providing the ci-VSP and dr-VSP clones, Drs. Nikita Gamper (University of Leeds) and Andrew Tinker (University College London) for providing the tubby-R332H-YFP clone, Dr. Xuming Zhang (Aston University, Birmingham, UK) for providing the $3G_{qiq}$ clone, and Linda Zabelka for maintaining the mouse colony.

ABSTRACT

Activation of G-protein coupled receptors (GPCRs) was proposed to inhibit the cold and menthol sensitive Transient Receptor Potential Melastatin 8 (TRPM8) channels via direct binding of $G_{\alpha q}$ to the channel. It is well documented that TRPM8 requires the plasma membrane phospholipid phosphatidylinositol 4,5-bisphosphate [$PI(4,5)P_2$ or PIP_2] for activity. It was claimed however that a decrease in cellular levels of this lipid does not contribute to channel inhibition upon receptor activation. Here we show that supplementing the whole cell patch pipette with $PI(4,5)P_2$ reduced inhibition of TRPM8 by activation of $G_{\alpha q}$-coupled receptors in mouse dorsal root ganglion (DRG) neurons. Activation of the same receptors induced Phospholipase C (PLC) activation and decreased plasma membrane $PI(4,5)P_2$ levels in these neurons. $PI(4,5)P_2$ also reduced inhibition of TRPM8 by activation of heterologously expressed $G_{\alpha q}$-coupled muscarinic M1 receptors. Co-expression of a constitutively active $G_{\alpha q}$ protein that does not couple to PLC inhibited TRPM8 activity, and in cells expressing this protein decreasing $PI(4,5)P_2$ levels using a voltage sensitive 5'-phosphatase induced a stronger inhibition of TRPM8 activity than in control cells. Our data indicate that $PI(4,5)P_2$ depletion plays an important role in TRPM8 inhibition upon GPCR activation, and $G_{\alpha q}$ inhibits the channel by reducing its apparent affinity for $PI(4,5)P_2$ and thus sensitizes the channel to inhibition by decreasing $PI(4,5)P_2$ levels.

INTRODUCTION

TRPM8 is a non-selective Ca^{2+} permeable cation channel activated by cold temperatures, as well as chemical agonists such as menthol, icilin, and WS12 (Almaraz et al., 2014). It is expressed in the primary sensory neurons of dorsal root ganglia (DRG) and trigeminal ganglia (TG), and mice lacking these channels display deficiencies in sensing moderately cold (Bautista et al., 2007; Colburn et al., 2007; Dhaka et al., 2007) as well as noxious cold temperatures (Knowlton et al., 2010). TRPM8 may also play a role in cold allodynia induced by nerve injury (Xing et al., 2007).

DRG neurons express receptors for various inflammatory mediators, such as bradykinin, ATP and prostaglandins. Most of those receptors couple to heterotrimeric G-proteins in the G_q family, and lead to activation of phospholipase C (PLC) (Rohacs, 2016). Activation of these G_q-coupled receptors induces thermal hyperalgesia (Caterina et al., 2000), via mechanisms including sensitizing the heat- and capsaicin-activated Transient Receptor Potential Vanilloid (TRPV1) channels (Cesare and McNaughton, 1996; Tominaga et al., 2001) and inhibiting the cold-activated TRPM8 channels (Premkumar et al., 2005; Zhang et al., 2012).

The mechanism of the inhibition of TRPM8 by G_q-coupled receptors is not fully understood. Protein Kinase C (PKC) has been proposed to be involved in sensitization of TRPV1 (Zhang et al., 2008), but its involvement in TRPM8 inhibition is controversial (Premkumar et al., 2005; Zhang et al., 2012). It was proposed that binding of $G_{\alpha q}$ to TRPM8 mediates inhibition of the channel (Zhang et al., 2012). Similar to most TRP channels (Rohacs, 2014), TRPM8 requires the membrane phospholipid phosphatidylinositol 4,5-bisphosphate [$PI(4,5)P_2$ or PIP_2] for activity (Liu and Qin, 2005; Rohacs et al., 2005; Daniels et al., 2009; Zakharian et al., 2010). Ca^{2+} influx through the channel was shown to activate a Ca^{2+} sensitive PLC isoform, and the resulting decrease in $PI(4,5)P_2$ levels limits

channel activity, leading to desensitization (Rohacs et al., 2005; Daniels et al., 2009; Yudin et al., 2011; Yudin et al., 2016). Stimulation of G_q-coupled receptors leads to the activation of PLCβ isoforms, which hydrolyze $PI(4,5)P_2$, but it was questioned whether this leads to a decrease in $PI(4,5)P_2$ levels in DRG neurons (Liu et al., 2010), and it was argued that a decrease in $PI(4,5)P_2$ levels does not play a role in TRPM8 channel inhibition (Zhang et al., 2012).

Here we revisited this question, and demonstrate that the decrease in $PI(4,5)P_2$ levels plays an important role in inhibition of TRPM8 by G_q-coupled receptor activation in DRG neurons. First we show that application of a cocktail of inflammatory mediators that activate G_q-coupled receptors decreased $PI(4,5)P_2$ levels and inhibited TRPM8 activity in DRG neurons. Supplementing the whole cell patch pipette with $PI(4,5)P_2$ alleviated the inhibition of TRPM8 by these receptor agonists. Excess $PI(4,5)P_2$ also decreased the inhibition of heterologously expressed TRPM8 by activation of muscarinic M1 receptors. Co-expression of a constitutively active $G_{\alpha q}$ that is deficient in PLC activation inhibited TRPM8 activity, which is consistent with earlier results (Zhang et al., 2012). Co-expression of $G_{\alpha q}$ also increased the sensitivity of TRPM8 inhibition by decreasing $PI(4,5)P_2$ levels using a specific voltage sensitive phosphoinositide 5-phosphatase, providing a mechanistic framework of how $G_{\alpha q}$ inhibits TRPM8. Overall, our data indicate that a decrease in $PI(4,5)P_2$ levels and direct binding of $G_{\alpha q}$ converge on inhibiting TRPM8 activity upon cell surface receptor activation.

MATERIALS AND METHODS

DRG neuron isolation and preparation

All animal procedures were approved by the Institutional Animal Care and Use Committee at Rutgers New Jersey Medical School. Dorsal root ganglion (DRG) neurons were isolated from 2- to 6-month-old wild-type C57BL6 or TRPM8-GFP mice (Takashima et al., 2007) as described previously (Yudin et al., 2016) with

some modifications. DRG neurons were isolated from mice of either sex anesthetized and perfused via the left ventricle with ice-cold Hank's buffered salt solution (HBSS; Invitrogen). DRGs were harvested from all spinal segments after laminectomy and removal of the spinal column and maintained in ice-cold HBSS for the duration of the isolation. Isolated ganglia were cleaned from excess dorsal root nerve tissue and incubated in an HBSS-based enzyme solution containing 3 mg/ml type I collagenase (Worthington) and 5 mg/ml Dispase (Sigma) at 37°C for 35 min, followed by mechanical trituration by repetitive pipetting through an uncut 1000 µl pipette tip. Digestive enzymes were then removed after centrifugation of the cells at 80 × g for 10 min. Cells were then either directly re-suspended in growth medium and seeded onto glass coverslips coated with a mixture of poly-D-lysine (Invitrogen) and laminin (Sigma), or were first transfected using the Amaxa nucleoporator according to manufacturer's instructions (Lonza Walkersville). Briefly, 60,000–100,000 cells obtained from each animal were re-suspended in 100 µl nucleofector solution or certain amount of transduction mix after complete removal of digestive enzymes. The cDNA used for transfecting neurons was prepared using the Endo-Free Plasmid Maxi Kit from QIAGEN. Vectors and reagent for transduction with the Green PIP_2 Sensor (CAG-Promoter) #D0405G were obtained from Montana Molecular. Before seeding onto glass coverslips, cells were transduced according to the manufacturers instructions. Neurons were maintained in culture for at least 24 h before measurements in DMEM-F12 supplemented with 10% FBS (Thermo Scientific), 100 IU/ml penicillin and 100 µg/ml streptomycin.

HEK cell culture and preparation

Human embryonic kidney 293 (HEK293) cells were obtained from the American Type Culture Collection (ATCC) (catalogue number CRL-1573) and were cultured in minimal essential medium (Invitrogen) containing supplements of 10% (v/v) Hyclone-characterized FBS (Thermo Scientific), 100 IU/ml penicillin, and 100 µg/ml streptomycin. Transient transfection was performed at ~70% cell

confluence with the Effectene reagent (QIAGEN) according to the manufacturer's protocol. Cells were incubated with the lipid–DNA complexes overnight (16-20 h). The cDNA used for transfecting HEK cells was prepared using the Endo-Free Plasmid Maxi Kit from QIAGEN. $3G_{qiq}$ cDNA was obtained from Xuming Zhang's laboratory (Zhang et al., 2012). $3G_{qiq}$Q209L was generated using the QuickChange Mutagenesis Kit (Agilent). Transduction was performed at ~70% cell confluence with BacMam green PIP_2 sensor with CAG promoter and BacMam M1 receptor (Montana Molecular) according to manufacturer's protocol. Cells were incubated with transduction mix overnight (16-24 h). We then trypsinized and re-plated the cells onto poly-D-lysine-coated glass coverslips and incubated them for an additional at least 2 h (in the absence of the transfection reagent) before measurement. All mammalian cells were kept in a humidity-controlled tissue-culture incubator maintaining 5% CO_2 at 37°C.

Electrophysiology

Whole-cell patch-clamp recordings were performed at room temperature (27–30°C) as described previously (Yudin et al., 2016). Patch pipettes were pulled from borosilicate glass capillaries (1.75 mm outer diameter, Sutter Instruments) on a P-97 pipette puller (Sutter Instrument) to a resistance of 4–6 MΩ. After formation of seals, the whole-cell configuration was established and currents were measured at a holding potential of −60 mV or with a voltage ramp protocol from -100 mV to +100 mV using an Axopatch 200B amplifier (Molecular Devices). Currents were filtered at 2 kHz using the low-pass Bessel filter of the amplifier and digitized using a Digidata 1440 unit (Molecular Devices). In some experiments, membrane potential pulses of indicated lengths to 100 mV were applied to activate the voltage-sensitive phosphatase (Ci-VSP), as described earlier (Velisetty et al., 2016). Measurements were conducted in solutions based on either Ca^{2+}-free (NCF) medium containing the following (in mM): 137 NaCl, 4 KCl, 1 $MgCl_2$, 5 HEPES, 5 MES, 10 glucose, 5 EGTA, pH adjusted to 7.4 with NaOH, or 2 mM Ca^{2+} (NCF) medium containing the following (in mM): 137 NaCl,

5 KCl, 1 $MgCl_2$, 10 HEPES, 10 glucose, 2 $CaCl_2$, pH adjusted to 7.4 with NaOH (Lukacs et al., 2013a). Intracellular solutions for DRG measurements (NIC-DRG) consisted of the following (in mM): 130 K-Gluconate, 10 KCl, 2 $MgCl_2$, 2 Na_2ATP, 0.2 Na_2GTP, 1.5 $CaCl_2$, 2.5 EGTA, 10 HEPES, pH adjusted to 7.25 with KOH. Intracellular solutions for HEK293 whole-cell measurements (NIC-HEK) consisted of the following (in mM): 130 KCl, 10 KOH, 3 $MgCl_2$, 2 Na_2ATP, 0.2 Na_2GTP, 0.2 $CaCl_2$, 2.5 EGTA, 10 HEPES, pH adjusted to 7.25 with KOH (Lukacs et al., 2013b). DiC_8 $PI(4,5)P_2$ was dissolved in NIC.

Ca^{2+} imaging

Ca^{2+} imaging measurements were performed with an Olympus IX-51 inverted microscope equipped with a DeltaRAM excitation light source (Photon Technology International). DRG neurons or HEK cells were loaded with 1 μM fura-2 AM (Invitrogen) for 50 min before the measurement at room temperature (27–30°C), and dual-excitation images at 340 nm and 380 nm were recorded with a Roper Cool-Snap digital CCD camera. Measurements were conducted in NCF solution supplemented with 2 mM $CaCl_2$. Image analysis was performed using the Image Master software (PTI).

Confocal fluorescence imaging

Confocal measurements were conducted with an Olympus FluoView-1000 confocal microscope operation in frame scan mode (Olympus) at room temperature (~25°C). GFP and YFP fluorescence (both excitation at 473 nm, emission at 520 nm) was recorded. DRG neurons or HEK cells were transfected with YFP-Tubby R332H-pcDNA3.1 or YFP-Tubby WT-pcDNA3.1 at least 24 hours before confocal measurements. Before each experiment, neurons or HEK cells were serum-deprived in Ca^{2+} free or 2 mM Ca^{2+}-containing NCF solution for at least 20 min. For transduction experiments, DRG neurons or HEK cells were transduced at least 24 hours before confocal measurements by BacMam green

$PI(4,5)P_2$ sensor with CAG promoter and BacMam M1 receptor. Before each experiment, neurons or HEK cells were serum-deprived in DPBS (Sigma-Aldrich) for 30 min in the dark. Image analysis was performed using Olympus FluoView-1000 and ImageJ.

Experimental Design and Statistical analysis

Data analysis was performed in Excel and Microcal Origin. Data collection was randomized. Data were analyzed with t-test, or Analysis of variance, p values are reported in the figures. Data are plotted as mean +/- standard error of the mean (SEM) for most experiments.

RESULTS

$PI(4,5)P_2$ alleviates inhibition of TRPM8 activity by G_q-coupled receptors in DRG neurons

Mouse DRG neurons express a number of different $G_{\alpha q}$-protein coupled receptors (Thakur et al., 2014). To identify receptors co-expressed with TRPM8, first we performed Ca^{2+} imaging experiments in DRG and TG neurons isolated from TRPM8-GFP reporter mice. We consecutively applied 500 μM menthol, 2 μM bradykinin, 1 μM prostaglandin E2 (PGE2), and 500 nM endothelin (ET) (Fig. S1 A, B). Most DRG neurons (62%) and TG neurons (84%) activated by menthol responded to either bradykinin, PGE2 or ET, but no individual agonist stimulated all TRPM8 positive neurons.

Next we measured Ca^{2+} signals in DRG neurons in response to the more specific TRPM8 agonist WS12 and to activate various $G_{\alpha q}$-coupled receptors we applied an inflammatory cocktail containing 100 μM ADP, 100 μM UTP, 500 nM bradykinin, 100 μM histamine, 100 μM serotonin, 10 μM PGE2 and 10 μM prostaglandin I2 (PGI2) (Fig. S1 C, D), similar to that used by (Zhang et al.,

2012). We found that 11% of all DRG neurons were GFP positive and 57% of GFP-positive neurons responded to WS12 (Fig. S1 E). Within these GFP positive neurons, almost all neurons activated by WS12 responded to the inflammatory cocktail. Only one neuron (out of 214 neurons) was stimulated by WS12 but not by the inflammatory cocktail (Fig. S1 C, D, E).

Next we preformed whole-cell patch clamp experiments on TRPM8-GFP reporter mouse DRG neurons and tested the effect of supplementing the patch pipette solution with the water-soluble diC_8 PI(4,5)P_2. We used a protocol of consecutive 1 min applications of 10 μM WS12 in Ca^{2+}-free NCF solution. Inflammatory cocktail was applied 1 min before the third application of WS12 (Fig. 1 A, B). Without diC_8 PI(4,5)P_2, current amplitudes induced by WS12 with inflammatory cocktail were reduced to 47% of currents induced by WS12 only (Fig. 1 A,C,D). When we included diC_8 PI(4,5)P_2 in the patch pipette solution, current amplitudes induced by WS12 with inflammatory cocktail were reduced only to 91% of currents induced by WS12 only (Fig. 1 B,C,D). These findings show TRPM8 channel activity is inhibited by $G_{\alpha q}$-protein coupled receptors in DRG neurons, and this inhibition is alleviated by excess PI(4,5)P_2.

Receptor-induced decrease of PI(4,5)P_2 in the plasma membrane

There are conflicting result on whether plasma membrane PI(4,5)P_2 levels decrease in DRG neurons in response to stimulating endogenous G_q-coupled bradykinin receptors (Liu et al., 2010; Lukacs et al., 2013b), and there is no information on the effects of other G_q-coupled receptors (Rohacs, 2016). Therefore we tested if there is a decrease in PI(4,5)P_2 levels in response to the inflammatory cocktail we used in our electrophysiology experiments. We transfected DRG neurons with the YFP-tagged R322H Tubby PI(4,5)P_2 sensor using the Amaxa nucleoporator system. This YFP-tagged phosphoinositide binding domain of the Tubby protein contains the R322H mutation that decreases its affinity for PI(4,5)P_2, thus increasing its sensitivity to small, physiological

decreases in $PI(4,5)P_2$ levels (Quinn et al., 2008; Lukacs et al., 2013b). The Tubby-based fluorescent sensor binds to $PI(4,5)P_2$ specifically; it is located in the plasma membrane in resting conditions; when $PI(4,5)P_2$ levels decrease, this indicator is translocated into the cytoplasm, which we monitored using confocal microscopy. Application of the inflammatory cocktail induced rapid translocation of the fluorescent sensor from the plasma membrane to the cytoplasm in the neuron cell body (Fig. 2 A, B, middle panels) as well as in the neuronal processes (Fig. 2 A, B, bottom panels), indicating decreased $PI(4,5)P_2$ levels. Figs. 2 C-E summarize these results.

We also monitored $PI(4,5)P_2$ levels using a different fluorescence based sensor the BacMam $PI(4,5)P_2$ sensor kit from Montana Molecular. This green $PI(4,5)P_2$ sensor is based on a dimerization-dependent fluorescent $PI(4,5)P_2$ binding protein (Tewson et al., 2013). The kit also contains cDNA for the M1 muscarinic receptor, a $G_{\alpha q}$-protein coupled receptor, to serve as a positive control (Thakur et al., 2014). Isolated neurons transduced with green BacMam $PI(4,5)P_2$ sensor showed prominent plasma membrane labeling. Administration of inflammatory cocktail induced robust decrease of fluorescence levels in the plasma membrane, indicating decreased $PI(4,5)P_2$ levels. Carbachol was applied at the end to activate M1 receptors, which induced a further decrease of fluorescence in most DRG neurons (Fig. 3 A-F).

We also tested receptor-induced depletion of $PI(4,5)P_2$ in HEK293 cells transduced with the green BacMam $PI(4,5)P_2$ sensor and BacMam M1 receptor. After 24-hour culture, HEK cells showed prominent plasma membrane labeling. Administration of carbachol in 2 mM Ca^{2+} NCF solution induced robust decrease of fluorescence levels in the plasma membrane, no changes were detected in "bleaching" control experiments (Fig. 3 G-L). Based on these results, we conclude that activation of G_q-coupled receptors decreases $PI(4,5)P_2$ levels in the plasma membrane.

$PI(4,5)P_2$ alleviates inhibition of TRPM8 activity by heterologously expressed G_q-coupled receptors

We showed that $PI(4,5)P_2$ alleviated inhibition of TRPM8 activity by G_q-coupled receptors in DRG neurons. Next we tested if this was reproducible in HEK293 cells co-expressing TRPM8 and M1 receptors, which were reported to inhibit TRPM8 (Li and Zhang, 2013). To this end, we performed whole-cell patch clamp experiments with, or without supplementing the patch pipette solution with the water-soluble diC_8 $PI(4,5)P_2$ (Fig. 4 A, B). First we used a protocol of consecutive 20-second applications of 200 μM menthol in Ca^{2+}-free NCF solution. Carbachol was applied 80 seconds before the fourth application of menthol. Current amplitudes induced by menthol were partially reduced by carbachol to 58% (at +60 mV) and 60% (at -60 mV) of currents induced by menthol only. When the patch pipette contained diC_8 $PI(4,5)P_2$, there was no decrease in current amplitudes after carbachol application (Fig. 4 D). We also tested whether protein kinase C (PKC) played a role in this inhibition. Previous studies showed controversial effects of PKC in TRPM8 inhibition induced by G_q-coupled receptors (Premkumar et al., 2005; Zhang et al., 2012). We co-applied the PKC inhibitor BIM IV (1 μM) with 100 μM carbachol for 80 seconds before the fourth application of menthol (Fig. 4 C). We found no significant effect of BIM IV (Fig. 4 D), similar to the findings of (Zhang et al., 2012).

Next we performed similar experiments in NCF solution containing 2 mM Ca^{2+} (Fig. 4 E-G). Upon application of carbachol, TRPM8 currents induced by menthol were reduced to 18% at +60 mV and 29% at -60 mV. The inhibition was partially rescued by adding diC_8 $PI(4,5)P_2$ into patch pipette solution; current levels decreased to 37% (at +60 mV) and 46% (at -60 mV) under these conditions (Fig. 4 G).

Next we examined whether the enhanced inhibition in the presence of extracellular Ca^{2+} was because of different levels of $PI(4,5)P_2$ depletion. We

transfected HEK293 cells with the YFP-tagged wild-type Tubby and M1 receptor, and monitored translocation with confocal microscopy. The YFP-tagged wild type Tubby has higher affinity for $PI(4,5)P_2$ than the YFP-tagged R322H Tubby (Quinn et al., 2008), therefore it may be more sensitive to changes at high levels of $PI(4,5)P_2$ depletion. HEK293 cells transfected with YFP-tagged WT tubby showed prominent plasma membrane labeling and application of 100 μM carbachol both in 2 mM Ca^{2+} NCF solution and in Ca^{2+}-free NCF solution induced translocation of fluorescent sensors from the plasma membrane to the cytoplasm (Fig. 5 A-E). Fluorescence levels in 2 mM Ca^{2+} NCF solution decreased more in plasma membrane and increased more in cytosol than in Ca^{2+}-free NCF solution (Fig. 5C) and this difference was statistically significant (Fig. 5E). This indicates that M1 receptor activation induced a larger decrease in $PI(4,5)P_2$ levels in the presence of extracellular Ca^{2+}, compared to that in the absence of extracellular Ca^{2+}. This correlates well with the stronger inhibition of TRPM8 in the presence of extracellular Ca^{2+}. We also used lower affinity YFP-tagged R322H Tubby in 2 mM Ca^{2+} NCF solution and in Ca^{2+} -free NCF solution and found that there was no significant difference of $PI(4,5)P_2$ level changes detected (Fig. S2 A-E). This is likely due to the large decrease of $PI(4,5)P_2$ levels in both conditions, differentiating between which is outside the dynamic range of this probe.

$G_{\alpha q}$ inhibits TRPM8 in the absence of PLC activation

$G_{\alpha q}$ is inactive in the GDP-bound form in resting cells, and active in the GTP-bound form upon receptor activation, when it binds to and activates phospholipase Cβ isoforms (PLCβ). $3G_{qiq}$ is a $G_{\alpha q}$ mutant that does not couple to PLC, and $3G_{qiq}$Q209L is a constitutive active Gαq mutant that also does not couple to PLC (Zhang et al., 2012). We used Fura2 AM to measure Ca^{2+} level changes upon menthol application in HEK293 cells co-expressed with TRPM8 and either $3G_{qiq}$ or $3G_{qiq}$Q209L (Fig. 6 A, B). Menthol-induced Ca^{2+} level increase was significantly less in cells with $3G_{qiq}$Q209L than in cells with wild $3G_{qiq}$ or TRPM8 only (Fig. 6 A-D). This is consistent with the whole-cell patch-

clamp results of Zhang et al. 2012, who found that $3G_{qiq}$Q209L inhibits TRPM8 activity and $3G_{qiq}$ does not.

PI(4,5)P_2 depletion inhibits TRPM8 more efficiently in the presence of $G_{\alpha q}$

To bypass the PLC pathway, we used a voltage-sensitive 5' phosphatase (Ci-VSP) to deplete PI(4,5)P_2 by converting it to PI(4)P (Iwasaki et al., 2008). Whole-cell patch-clamp experiments were performed in HEK293 cells co-transfected with TRPM8 and Ci-VSP, with or without $3G_{qiq}$Q209L in Ca^{2+}-free NCF solution (Fig. 7 A-D). Ci-VSP was activated by depolarizing pulses to 100 mV for 0.1 s, 0.2 s, 0.3 s, and 1 s; menthol-induced currents were gradually reduced to 85%, 66%, 51%, and 32% respectively in cells without $3G_{qiq}$Q209L. In cells expressing $3G_{qiq}$Q209L, the same depolarizing pulses induced larger reductions in menthol-evoked currents, to 32%, 20%, 18%, and 15% respectively (Fig. 7 D). These results indicate that TRPM8 is inhibited more by PI(4,5)P_2 depletion in the presence of $G_{\alpha q}$.

We conclude that PI(4,5)P_2 alleviates inhibition of TRPM8 activity by G_q-coupled receptors in DRG neurons. $G_{\alpha q}$ not only directly inhibits TRPM8 as proposed by Zhang et al 2012, but also sensitizes the channel to inhibition by decreasing PI(4,5)P_2 levels, therefore the two pathways converge to inhibit TRPM8 activity upon GPCR activation.

DISCUSSION

Converging evidence demonstrate that TRPM8 channels require the plasma membrane phospholipid PI(4,5)P_2 for activity. TRPM8 currents show a characteristic decrease (rundown) in excised inside out patches, which can be restored by applying PI(4,5)P_2 to the cytoplasmic surface of the membrane patch (Liu and Qin, 2005; Rohacs et al., 2005). Increasing endogenous PI(4,5)P_2 levels with MgATP also restored TRPM8 activity in excised patches after current

rundown (Yudin et al., 2011). $PI(4,5)P_2$ is also required for the cold- or menthol-induced activity of the purified TRPM8 protein in planar lipid bilayers, indicating a direct effect on the channel (Zakharian et al., 2009; Zakharian et al., 2010). $PI(4,5)P_2$ was also shown to modulate the cold threshold of the channel (Fujita et al., 2013). In accordance with dependence of the activity of TRPM8 on $PI(4,5)P_2$, it was shown that selectively decreasing $PI(4,5)P_2$ levels in intact cells is sufficient to inhibit channel activity either by using specific chemically inducible phosphoinositide phosphatases (Varnai et al., 2006; Daniels et al., 2009), or voltage sensitive phosphatases such as ciVSP (Yudin et al., 2011).

Stimulating cell surface receptors that couple to $G_{\alpha q}$ and activate PLC inhibits TRPM8 activity (Liu and Qin, 2005; Premkumar et al., 2005; Zhang et al., 2012; Li and Zhang, 2013; Than et al., 2013). Based on the following arguments it was proposed that this inhibition proceeds via direct binding of $G_{\alpha q}$ to the channel (Zhang et al., 2012). Application of $G_{\alpha q}$ and GTPγS inhibited TRPM8 activity in excised inside out patches in the presence of $PI(4,5)P_2$. Direct binding of $G_{\alpha q}$ to TRPM8 was demonstrated by immunoprecipitation. Co-expression of a constitutively active mutant (Q209L) chimera between $G_{\alpha i}$ and $G_{\alpha q}$ ($3G_{\alpha qiq}$) that does not activate PLC inhibited TRPM8 activity (Zhang et al., 2012).

It was also proposed that decreasing $PI(4,5)P_2$ levels do not contribute to TRPM8 inhibition by G_q-coupled receptors (Zhang et al., 2012) based on the following data: Histamine inhibited TRPM8 in the presence of the PLC inhibitor U73122. The inhibition however was less that without the drug, indicating potential involvement of PLC activation. Two mutants in the putative TRP domain were also tested, and the authors argued that since these "$PI(4,5)P_2$ insensitive" TRPM8 mutants were inhibited by GPCR activation, $PI(4,5)P_2$ depletion is not involved. These mutants however are more sensitive to $PI(4,5)P_2$ depletion, due to their decreased apparent affinity for the lipid (Rohacs et al., 2005), and indeed the K995Q mutant was somewhat more inhibited by histamine than wild-type TRPM8, and the extent of inhibition for the R1008Q is difficult to evaluate due to

the very small current amplitudes (Zhang et al., 2012). Finally, the constitutively active Q209L mutant of the $3G\alpha_{qiq}$ chimera that does not activate PLC inhibited TRPM8 activity when co-expressed in HEK cells. The inhibition however was substantially smaller than that induced by the constitutively active $G_{\alpha q}$ indicating PLC dependent mechanisms may also involved (Zhang et al., 2012). In conclusion, most of the data discussed here is compatible with $PI(4,5)P_2$ depletion contributing to TRPM8 inhibition.

To test the involvement of $PI(4,5)P_2$ depletion, we supplemented the whole cell patch pipette with the lipid, and found that this maneuver alleviated inhibition of TRPM8 activity by G_q-coupled receptor activation both in DRG neurons, and in an expression system. In DRG neurons, we used an inflammatory cocktail, similar to that used by (Zhang et al., 2012) for two reasons. First, DRG neurons are highly heterogenous, and we could not find a single agonist that reliably induced a Ca^{2+} signal indicating PLC activation in all TRPM8 positive neurons. Second, inflammation is mediated not by a single pro-inflammatory agonist, but rather a combination of them, which is sometime referred to as an “inflammatory soup”.

While activation of PLC induces $PI(4,5)P_2$ hydrolysis, the extent to which $PI(4,5)P_2$ is decreased is debated (Nasuhoglu et al., 2002), and is clearly cell type and agonist specific (van der Wal et al., 2001). Liu et al., using a fluorescent $PI(4,5)P_2$ sensor, the YFP-tagged $PI(4,5)P_2$ binding domain of the tubby protein (Quinn et al., 2008), showed that bradykinin activated PLC in rat DRG neurons, but it did not decrease in $PI(4,5)P_2$ levels (Liu et al., 2010). Our earlier data using the same sensor show that bradykinin induced a small decrease in $PI(4,5)P_2$ levels in mouse DRG neurons (Lukacs et al., 2013b). Here we demonstrate that application of the same inflammatory G_q-activating cocktail we used in our patch clamp measurements decreased $PI(4,5)P_2$ levels in a substantial portion of DRG neurons, using the tubby-based $PI(4,5)P_2$ sensor. Note that this decrease was smaller than that induced by activating heterologously expressed M1 receptors

therefore in native cells, additional mechanisms may be needed to induce substantial inhibition of TRPM8 activity.

We found that co-expressing the PLC deficient constitutively active $3G\alpha_{qiq}$-Q209L inhibited menthol-induced Ca^{2+} signals in HEK cells expressing TRPM8, confirming the results of (Zhang et al., 2012). We also found that the presence of $3G\alpha_{qiq}$-Q209L markedly increased the sensitivity of inhibition of TRPM8 by decreasing $PI(4,5)P_2$ levels with the voltage sensitive phosphoinositide 5-phosphatase ciVSP. These results indicate the $G_{\alpha q}$ binding to the channel decreases the apparent affinity of the channel for $PI(4,5)P_2$. It is quite likely that this decreased sensitivity to $PI(4,5)P_2$ would render basal $PI(4,5)P_2$ levels to be less efficient in maintaining channel activity, thus explaining the reduced TRPM8 current levels upon $G_{\alpha q}$ binding. This decreased apparent affinity would also allow even small decreases in $PI(4,5)P_2$ concentrations, such as those occurring during physiological receptor activation, to inhibit channel activity.

Overall we conclude that upon receptor activation, direct binding of $G_{\alpha q}$ not only directly inhibits TRPM8, but also sensitizes it to $PI(4,5)P_2$ depletion, and thus the two pathways converge and synergize in reducing channel activity.

REFERENCES

Almaraz, L., Manenschijn, J.A., de la Pena, E., and Viana, F. (2014). Trpm8. *Handb Exp Pharmacol 222*, 547-579.

Bautista, D.M., Siemens, J., Glazer, J.M., Tsuruda, P.R., Basbaum, A.I., Stucky, C.L., Jordt, S.E., and Julius, D. (2007). The menthol receptor TRPM8 is the principal detector of environmental cold. *Nature 448*, 204-208.

Caterina, M.J., Leffler, A., Malmberg, A.B., Martin, W.J., Trafton, J., Petersen-Zeitz, K.R., Koltzenburg, M., Basbaum, A.I., and Julius, D. (2000). Impaired nociception and pain sensation in mice lacking the capsaicin receptor. *Science 288*, 306-313.

Cesare, P., and McNaughton, P. (1996). A novel heat-activated current in nociceptive neurons and its sensitization by bradykinin. *Proc Natl Acad Sci U S A 93*, 15435-15439.

Colburn, R.W., Lubin, M.L., Stone, D.J., Jr., Wang, Y., Lawrence, D., D'Andrea, M.R., Brandt, M.R., Liu, Y., Flores, C.M., and Qin, N. (2007). Attenuated cold sensitivity in TRPM8 null mice. *Neuron 54*, 379-386.

Daniels, R.L., Takashima, Y., and McKemy, D.D. (2009). Activity of the neuronal cold sensor TRPM8 is regulated by phospholipase C via the phospholipid phosphoinositol 4,5-bisphosphate. *J Biol Chem 284*, 1570-1582.

Dhaka, A., Murray, A.N., Mathur, J., Earley, T.J., Petrus, M.J., and Patapoutian, A. (2007). TRPM8 is required for cold sensation in mice. *Neuron 54*, 371-378.

Fujita, F., Uchida, K., Takaishi, M., Sokabe, T., and Tominaga, M. (2013). Ambient temperature affects the temperature threshold for TRPM8 activation through interaction of phosphatidylinositol 4,5-bisphosphate. *J Neurosci 33*, 6154-6159.

Iwasaki, H., Murata, Y., Kim, Y., Hossain, M.I., Worby, C.A., Dixon, J.E., McCormack, T., Sasaki, T., and Okamura, Y. (2008). A voltage-sensing phosphatase, Ci-VSP, which shares sequence identity with PTEN, dephosphorylates phosphatidylinositol 4,5-bisphosphate. *Proc Natl Acad Sci U S A 105*, 7970-7975.

Knowlton, W.M., Bifolck-Fisher, A., Bautista, D.M., and McKemy, D.D. (2010). TRPM8, but not TRPA1, is required for neural and behavioral responses to acute noxious cold temperatures and cold-mimetics in vivo. *Pain 150*, 340-350.

Li, L., and Zhang, X. (2013). Differential inhibition of the TRPM8 ion channel by Galphaq and Galpha 11. *Channels (Austin) 7*, 115-118.

Liu, B., Linley, J.E., Du, X., Zhang, X., Ooi, L., Zhang, H., and Gamper, N. (2010). The acute nociceptive signals induced by bradykinin in rat sensory neurons are mediated by inhibition of M-type K+ channels and activation of Ca2+-activated Cl- channels. *J Clin Invest 120*, 1240-1252.

Liu, B., and Qin, F. (2005). Functional control of cold- and menthol-sensitive TRPM8 ion channels by phosphatidylinositol 4,5-bisphosphate. *J Neurosci 25*, 1674-1681.

Lukacs, V., Rives, J.M., Sun, X., Zakharian, E., and Rohacs, T. (2013a). Promiscuous activation of transient receptor potential vanilloid 1 channels by negatively charged intracellular lipids, the key role of endogenous

phosphoinositides in maintaining channel activity. *J Biol Chem 288*, 35003-35013.

Lukacs, V., Yudin, Y., Hammond, G.R., Sharma, E., Fukami, K., and Rohacs, T. (2013b). Distinctive changes in plasma membrane phosphoinositides underlie differential regulation of TRPV1 in nociceptive neurons. *Journal of Neuroscience 33*, 11451-11463.

Nasuhoglu, C., Feng, S., Mao, Y., Shammat, I., Yamamato, M., Earnest, S., Lemmon, M., and Hilgemann, D.W. (2002). Modulation of cardiac PIP2 by cardioactive hormones and other physiologically relevant interventions. *Am J Physiol Cell Physiol 283*, C223-234.

Premkumar, L.S., Raisinghani, M., Pingle, S.C., Long, C., and Pimentel, F. (2005). Downregulation of transient receptor potential melastatin 8 by protein kinase C-mediated dephosphorylation. *J Neurosci 25*, 11322-11329.

Quinn, K.V., Behe, P., and Tinker, A. (2008). Monitoring changes in membrane phosphatidylinositol 4,5-bisphosphate in living cells using a domain from the transcription factor tubby. *J Physiol 586*, 2855-2871.

Rohacs, T. (2014). Phosphoinositide regulation of TRP channels. *Handb Exp Pharmacol 233*, 1143-1176.

Rohacs, T. (2016). Phosphoinositide signaling in somatosensory neurons. *Adv Biol Regul 61*, 2-16.

Rohacs, T., Lopes, C.M., Michailidis, I., and Logothetis, D.E. (2005). PI(4,5)P2 regulates the activation and desensitization of TRPM8 channels through the TRP domain. *Nat Neurosci 8*, 626-634.

Takashima, Y., Daniels, R.L., Knowlton, W., Teng, J., Liman, E.R., and McKemy, D.D. (2007). Diversity in the neural circuitry of cold sensing revealed by genetic axonal labeling of transient receptor potential melastatin 8 neurons. *J Neurosci 27*, 14147-14157.

Tewson, P.H., Quinn, A.M., and Hughes, T.E. (2013). A multiplexed fluorescent assay for independent second-messenger systems: decoding GPCR activation in living cells. *J Biomol Screen 18*, 797-806.

Thakur, M., Crow, M., Richards, N., Davey, G.I., Levine, E., Kelleher, J.H., Agley, C.C., Denk, F., Harridge, S.D., and McMahon, S.B. (2014). Defining the nociceptor transcriptome. *Front Mol Neurosci 7*, 87.

Than, J.Y., Li, L., Hasan, R., and Zhang, X. (2013). Excitation and modulation of TRPA1, TRPV1, and TRPM8 channel-expressing sensory neurons by the pruritogen chloroquine. *J Biol Chem 288*, 12818-12827.

Tominaga, M., Wada, M., and Masu, M. (2001). Potentiation of capsaicin receptor activity by metabotropic ATP receptors as a possible mechanism for ATP-evoked pain and hyperalgesia. *Proc Natl Acad Sci U S A 98*, 6951-6956.

van der Wal, J., Habets, R., Varnai, P., Balla, T., and Jalink, K. (2001). Monitoring agonist-induced phospholipase C activation in live cells by fluorescence resonance energy transfer. *J Biol Chem 276*, 15337-15344.

Varnai, P., Thyagarajan, B., Rohacs, T., and Balla, T. (2006). Rapidly inducible changes in phosphatidylinositol 4,5-bisphosphate levels influence multiple regulatory functions of the lipid in intact living cells. *J Cell Biol 175*, 377-382.

Velisetty, P., Borbiro, I., Kasimova, M.A., Liu, L., Badheka, D., Carnevale, V., and Rohacs, T. (2016). A molecular determinant of phosphoinositide affinity in mammalian TRPV channels. *Sci Rep 6*, 27652.

Xing, H., Chen, M., Ling, J., Tan, W., and Gu, J.G. (2007). TRPM8 mechanism of cold allodynia after chronic nerve injury. *J Neurosci 27*, 13680-13690.

Yudin, Y., Lukacs, V., Cao, C., and Rohacs, T. (2011). Decrease in phosphatidylinositol 4,5-bisphosphate levels mediates desensitization of the cold sensor TRPM8 channels. *J Physiol 589*, 6007-6027.

Yudin, Y., Lutz, B., Tao, Y.X., and Rohacs, T. (2016). Phospholipase C delta4 regulates cold sensitivity in mice. *J Physiol 594*.

Zakharian, E., Cao, C., and Rohacs, T. (2010). Gating of transient receptor potential melastatin 8 (TRPM8) channels activated by cold and chemical agonists in planar lipid bilayers. *J Neurosci 30*, 12526-12534.

Zakharian, E., Thyagarajan, B., French, R.J., Pavlov, E., and Rohacs, T. (2009). Inorganic polyphosphate modulates TRPM8 channels. *PLoS One 4*, e5404.

Zhang, X., Li, L., and McNaughton, P.A. (2008). Proinflammatory mediators modulate the heat-activated ion channel TRPV1 via the scaffolding protein AKAP79/150. *Neuron 59*, 450-461.

Zhang, X., Mak, S., Li, L., Parra, A., Denlinger, B., Belmonte, C., and McNaughton, P.A. (2012). Direct inhibition of the cold-activated TRPM8 ion channel by Galpha(q). *Nat Cell Biol 14*, 851-858.

FIGURE LEGENDS

Figure 1. Intracellular dialysis of $PI(4,5)P_2$ alleviates inhibition of TRPM8 activity by G_q-coupled receptors in DRG neurons. ***A, B*****,** Representative whole-cell voltage-clamp traces of inward currents recorded at -60 mV from isolated DRG neurons. Measurements were conducted in Ca^{2+}-free NCF solution. Control-no lipid supplement (***A***), 100 μM diC_8 $PI(4,5)P_2$ supplement (***B***). 10 μM WS12 was applied to activate TRPM8 channels for 4 times. Cocktail containing 100 μM ADP, 100 μM UTP, 500 nM bradykinin, 100 μM histamine, 100 μM serotonin, 10 μM PGE2, 10 μM PGI2 was applied to activate various G_q-coupled receptors. ***C, D*****,** Statistical analysis of n=7 neurons (control group) and n=8 neurons (diC_8 $PI(4,5)P_2$ group) displayed. Bars represent mean ± SEM; statistical significance was calculated with two-way analysis of variance. Four peaks of current responses in each group were analyzed. Current values were normalized to the peak of the second current response in each group in ***D***.

Figure 2. Receptor-induced decrease of $PI(4,5)P_2$ in the plasma membrane of DRG neurons. ***A,*** Confocal images of wild type mouse DRG neurons transfected with YFP-tagged R322H Tubby domain as reporters of plasma membrane $PI(4,5)P_2$. Images are representatives of reporter distribution before and after application of either inflammatory cocktail or control solution (2 mM Ca^{2+} NCF). Measurements were conducted in 2 mM Ca^{2+} NCF solution. Neurons were serum-deprived in 2 mM Ca^{2+} NCF solution for 20 min. ***B,*** Graphs correspond to fluorescence intensities plotted along the lines indicated in each image in ***A*** before (red) and after (black) application of cocktail or control. ***C, D,*** Time courses of fluorescence density changes for YFP-tagged R322H Tubby in response to control solution (***C***) or inflammatory cocktail (***D***) in plasma membrane and cytosol of neuron cell body. ***E,*** Statistical analysis of fluorescence density right before and 1 min after application of inflammatory cocktail (n=14) and control solution (n=3) displayed. Bars represent mean ± SEM; statistical significance was calculated with two-way analysis of variance. Fluorescence

density values were normalized to the time point of right before application of inflammatory cocktail or control solution for each group.

Figure 3. Receptor-induced decrease of $PI(4,5)P_2$ in DRG neurons and HEK cells. ***A,*** Confocal images of wild type mouse DRG neurons tranducted with Green $PI(4,5)P_2$ sensor BacMam and human muscarinic cholinergic receptor 1 (M1). Images are representatives of reporter distribution before and after application of either cocktail or control solution (2 mM Ca^{2+} NCF). Measurements were conducted in 2 mM Ca^{2+} NCF solution. ***B,*** Graphs correspond to fluorescence intensities plotted along the lines indicated in each image in ***A*** before (red) and after (black) application of cocktail or control. ***C,*** Representative traces of time course changes for Green $PI(4,5)P_2$ sensor BacMam in response to cocktail followed by 100 μM carbachol in DRG neurons. ***D,*** Averaged time course of fluorescence density changes for Green $PI(4,5)P_2$ sensor BacMam in response to cocktail followed by 100 μM carbachol in DRG neurons. **E,** Statistical analysis of fluorescence density at baseline, 40 seconds after application of cocktail, right before application of carbachol and 40 seconds after application of carbachol in neurons (n=22). Bars represent mean ± SEM; statistical significance was calculated with two-way analysis of variance. Fluorescence density values were normalized to baseline. ***F,*** Time course of fluorescence density changes for Green $PI(4,5)P_2$ sensor BacMam in response to two applications of control solution (2 mM Ca^{2+} NCF) in DRG neurons (n=12). ***G,*** Confocal images of HEK cells transduced with Green $PI(4,5)P_2$ sensor BacMam as reporters of $PI(4,5)P_2$ and human muscarinic receptor 1 (M1) receptor. Images are representatives of reporter distribution before and after application of either 100 μM carbachol or control solution (2 mM Ca^{2+} NCF). Measurements were conducted in 2 mM Ca^{2+} NCF solution. ***H,*** Graphs correspond to fluorescence intensities plotted along the lines indicated in each image in ***G*** before (red) and after (black) application of 100 μM carbachol or control. ***I,*** Representative traces of time course changes for Green $PI(4,5)P_2$ sensor BacMam in response to carbachol. ***J, K,*** Average time course of fluorescence density changes for Green $PI(4,5)P_2$ sensor BacMam in

response to carbachol or control (2 mM Ca^{2+} NCF) in HEK cells. **L,** Statistical analysis of fluorescence density at baseline and after application of carbachol (n=18) or control (n=11). Bars represent mean ± SEM; statistical significance was calculated with two-way analysis of variance. Fluorescence density values were normalized to baseline

Figure 4. Intracellular dialysis of $PI(4,5)P_2$ alleviates inhibition of TRPM8 activity by G_q-coupled receptors in HEK cells. ***A, B, C,*** Representative whole-cell voltage-clamp traces of inward currents recorded at -60 mV and + 60 mV in Ca^{2+}-free NCF solution for HEK cells transfected with TRPM8 channels and M1 receptors. Control-no lipid supplement (***A, C***), 100 μM $diC_8PI(4,5)P_2$ supplement (***B***). 200 μM Menthol was applied to activate TRPM8 channels for 6 times. 100 μM carbachol and 1 μM BIM were applied to activate M1 receptor or inhibit protein kinase C (***C***), respectively. ***D,*** Statistical analysis of n=12 neurons (control), n=7 (diC_8 $PI(4,5)P_2$) and n=4 neurons (BIM) both at -60 mV and + 60 mV (corresponding to panel ***A, B, C***) displayed. Bars represent mean ± SEM; statistical significance was calculated with two-way analysis of variance. Current values were normalized to the 3rd current response to menthol (labeled as 1). The 4th current response to menthol with co-application of carbachol was labeled as 2A, 2B, 2C in groups of control, diC_8 $PI(4,5)P_2$ and BIM separately. ***E, F,*** Representative whole-cell voltage-clamp traces of inward currents recorded at –60 mV and + 60 mV in 2 mM Ca^{2+} NCF solution for HEK cells transfected with TRPM8 channels and M1 receptors; the applications of 200 μM Menthol and 100 μM carbachol were indicated by the horizontal lines; 100 μM diC_8 $PI(4,5)P_2$ was added into NIC in ***F***, no lipid solutions was added into NIC in ***E***. ***G,*** Statistical analysis of n=14 neurons (control) and n=13 (diC_8 $PI(4,5)P_2$) both at -60 mV and +60 mV (corresponding to panel ***E, F***) displayed. Bars represent mean ± SEM. *p<0.05 (two-sample Student's *t* test). Current values at the time point of 1.5 min after application of carbachol were analyzed. Current values were normalized to the peak current value under menthol application before carbachol.

Figure 5. Receptor-induced depletion of $PI(4,5)P_2$ in the plasma membrane of HEK cells in the presence or absence of calcium. ***A,*** Confocal images of HEK cells transfected with YFP-tagged wild type Tubby domain as reporters of plasma membrane phosphoinositides and M1 receptor in 2 mM Ca^{2+} NCF or Ca^{2+} -free NCF solution. Images are representatives of reporter distribution before and after application of either 100 μM carbachol or control solution (2 mM Ca^{2+} NCF). ***B,*** Graphs correspond to fluorescence intensities plotted along the lines indicated in each image in ***A*** before (red) and after (black) application of carbachol or control. ***C, D,*** Time courses of fluorescence density changes for YFP-tagged WT Tubby in response to carbachol (***C***) or control (***D***) in plasma membrane and cytosol of HEK cells. ***E,*** Statistical analysis of fluorescence density at baseline and at the end after application of carbachol (n=25 for 2 mM Ca^{2+} NCF , n=28 for Ca^{2+} -free NCF) and control (n=8) displayed. Bars represent mean ± SEM; statistical significance was calculated with two-way analysis of variance. Fluorescence density values were normalized to the baseline for each group.

Figure 6. TRPM8 is inhibited by $G_{\alpha q}$ when PLC is not activated. ***A,*** Calcium imaging measurements (mean ± SEM) of HEK cells transfected with TRPM8, plus 3GqiqQ209L or 3Gqiq in response to two applications of 200 μM Menthol. ***B,*** Pooled data of ***A*** normalized to baseline. ***C, D,*** corresponds to ***A*** and ***B,*** separately. Bars represent mean ± SEM; statistical significance was calculated with two-way analysis of variance. Fluorescence values of 340/380 ratio were normalized to the baseline for each group. Two peaks of menthol responses were analyzed. TRPM8 group (n=4 slides, including 103 cells), TRPM8+3GqiqQ209L group (n=5 slides, including 84 cells), TRPM8 + 3Gqiq group (n=4 slides, including 103 cells)

Figure 7. TRPM8 is inhibited more efficiently by $PI(4,5)P_2$ depletion in the presence of $G_{\alpha q}$. ***A, B,*** Representative whole-cell voltage-clamp traces of inward currents recorded at -60 mV from HEK cells transfected with TRPM8 and the voltage sensitive phosphatase CiVSP (***A***), or with ciVSP, TRPM8 and

3GqiqQ209L (***B***). Measurements were conducted in Ca^{2+}-free NCF solution. TRPM8 channels were activated by 500 μM menthol. CiVSP was activated by +100 mV steps for 0.1, 0.2, 0.3 and 1 second. ***C, D***, Statistical analysis of ***A*** and ***B*** displayed. Bars represent mean ± SEM; statistical significance was calculated with two-sample Student's *t* test , two-way analysis of variance. Current peak and current density upon voltage steps to +100 mV for 0.1, 0.2, 0.3 and 1 second were analyzed for each group (TRPM8 + CiVSP, n=7; TRPM8 + CiVSP + 3GqiqQ209L, n=9) in ***C***. Relative currents were analyzed upon voltage steps to +100 mV for 0.1, 0.2, 0.3 and 1 second in ***D***.

Figure 1

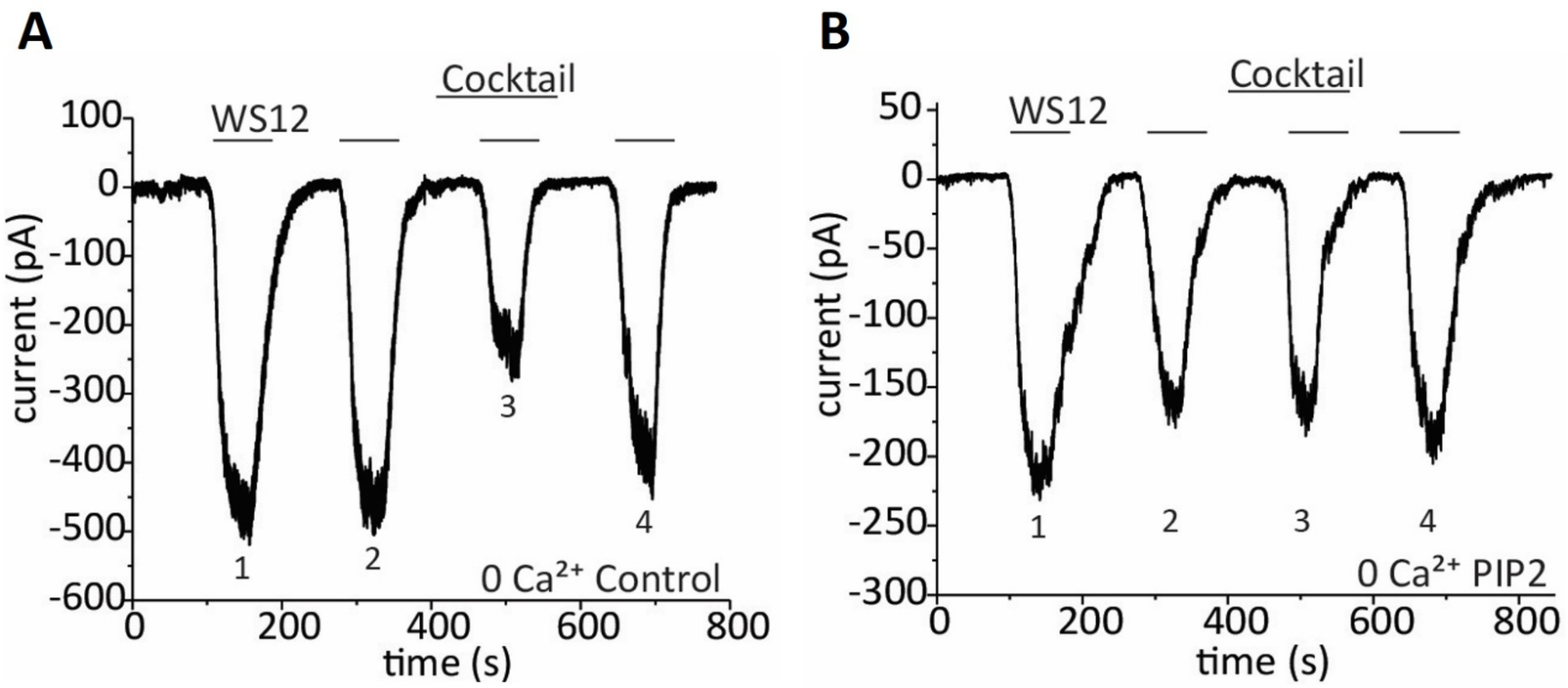

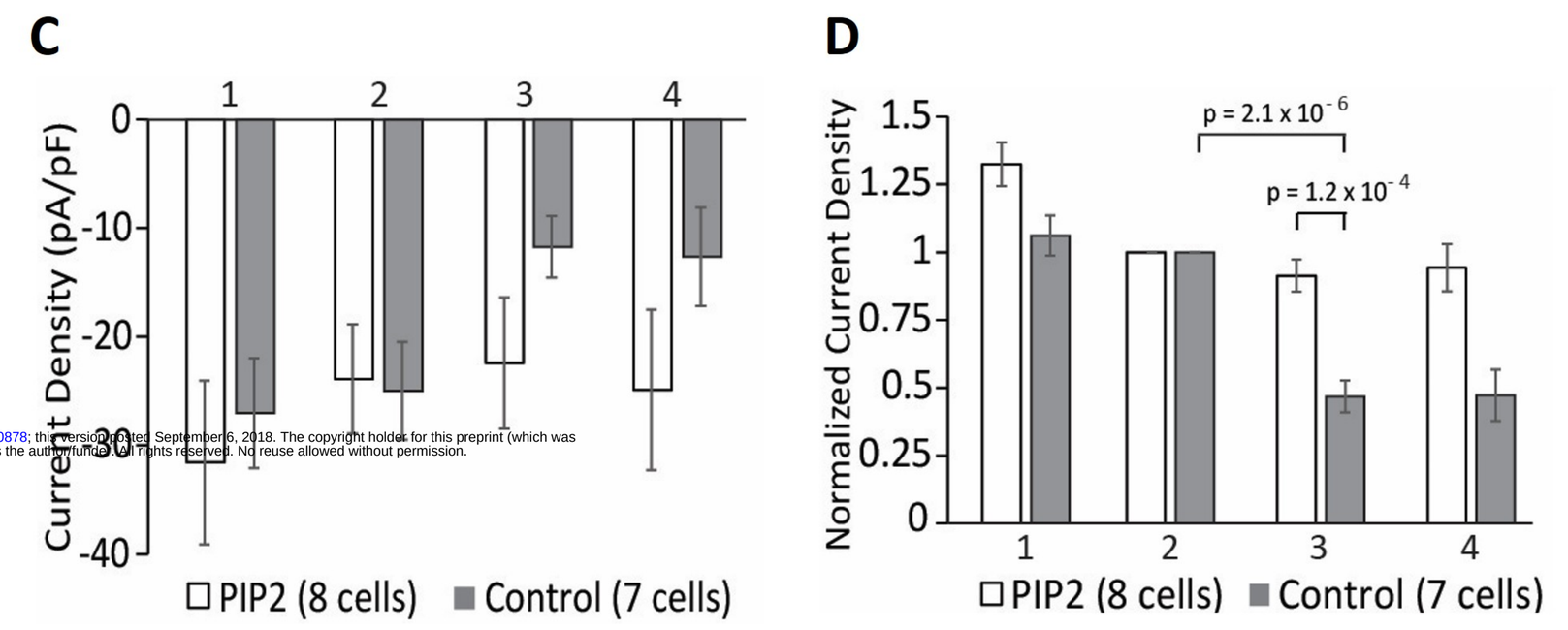

Figure 2

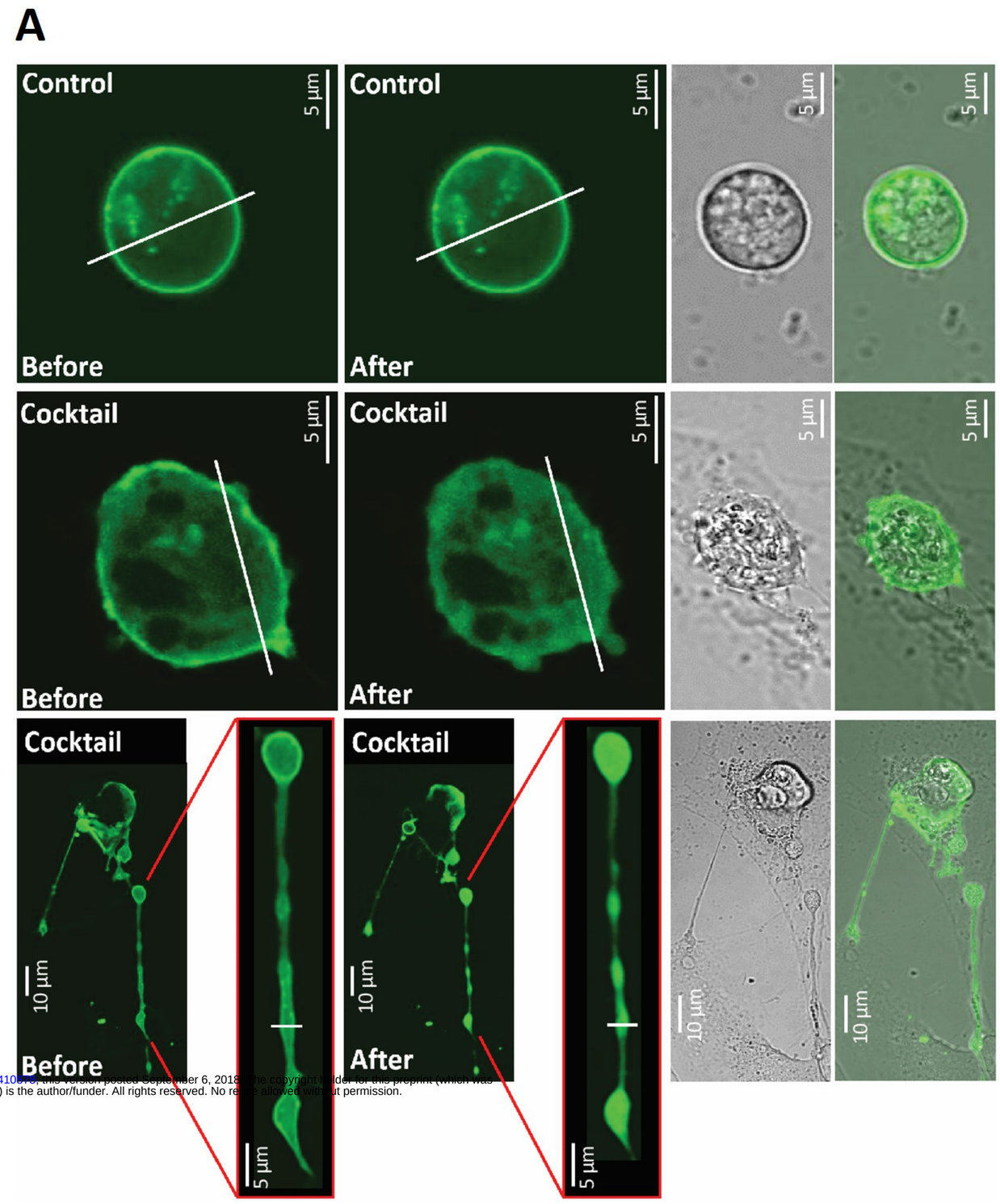

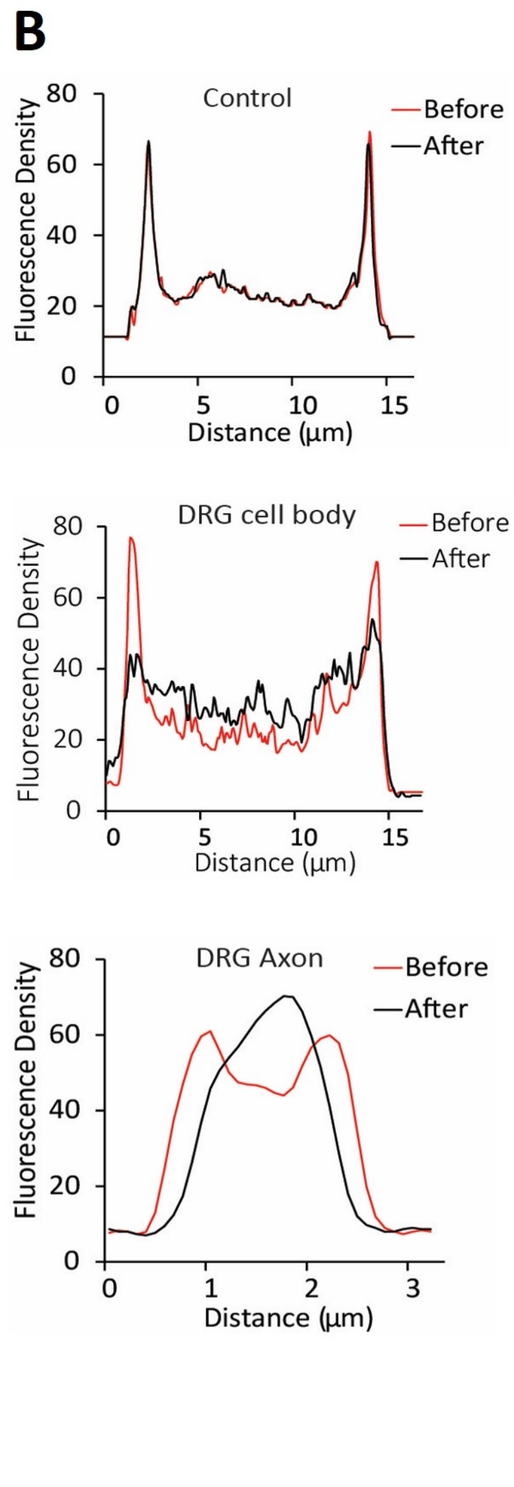

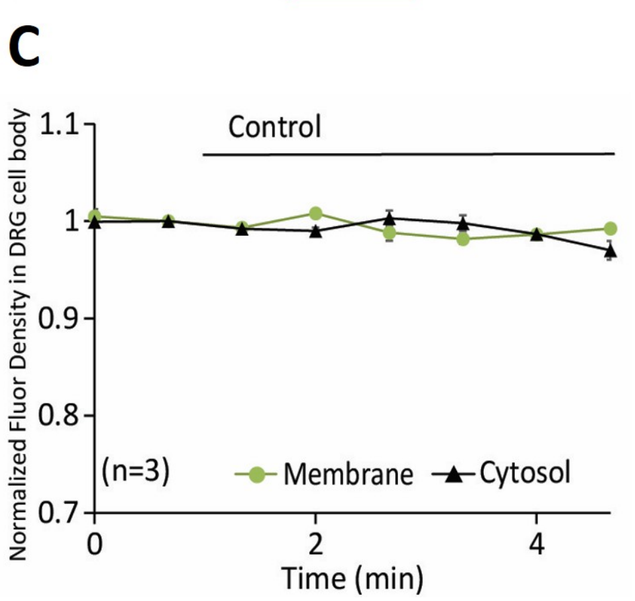

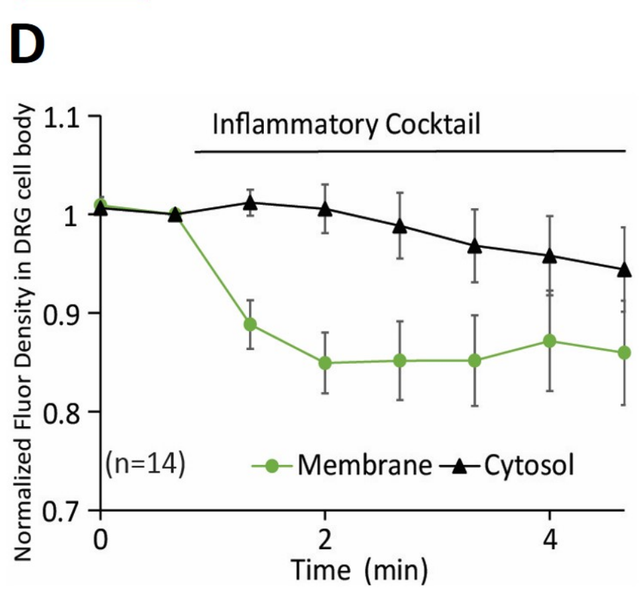

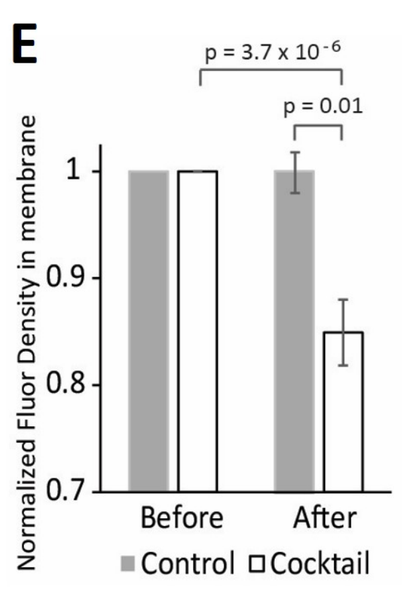

Figure 3

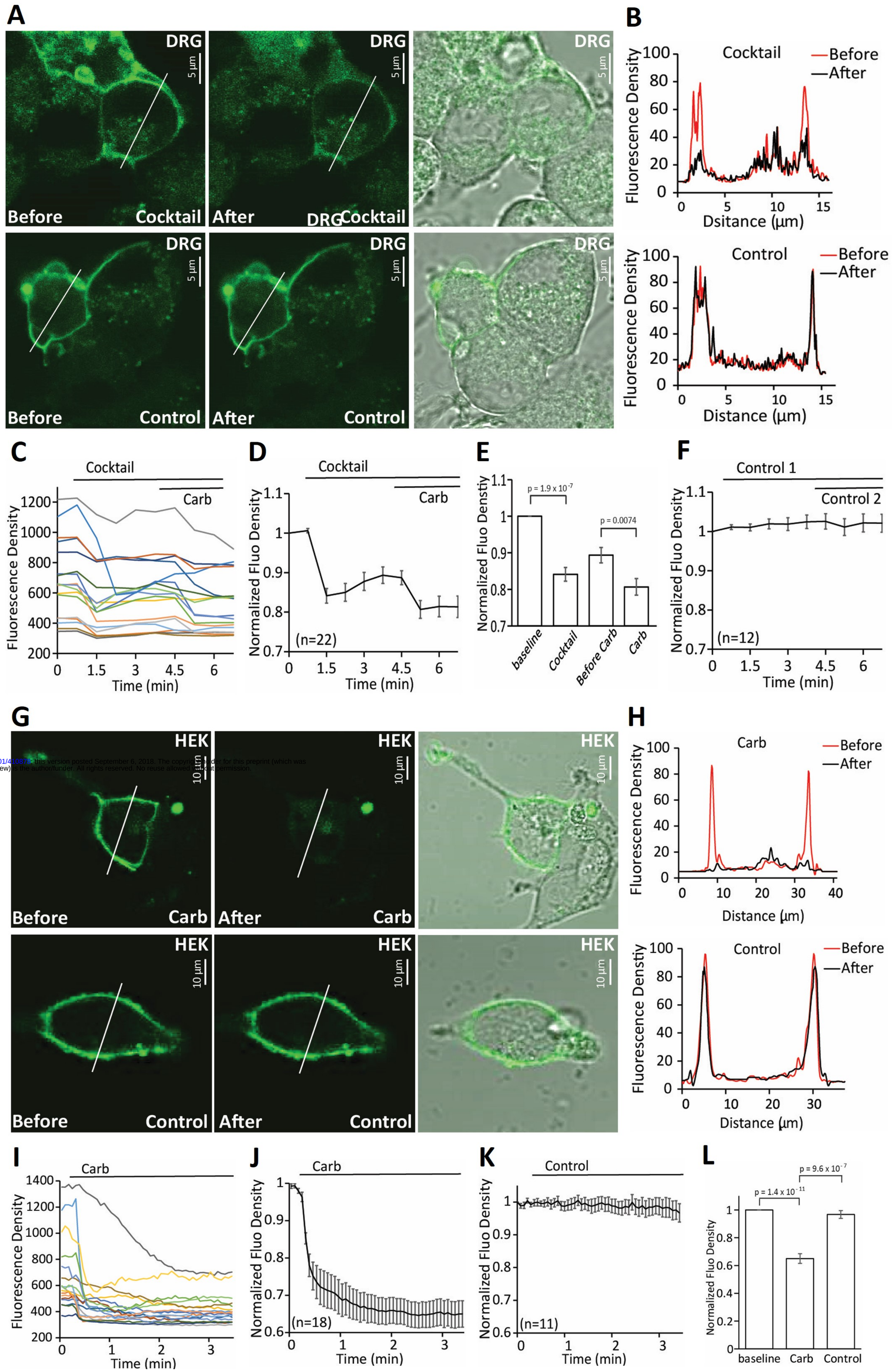

Figure 4

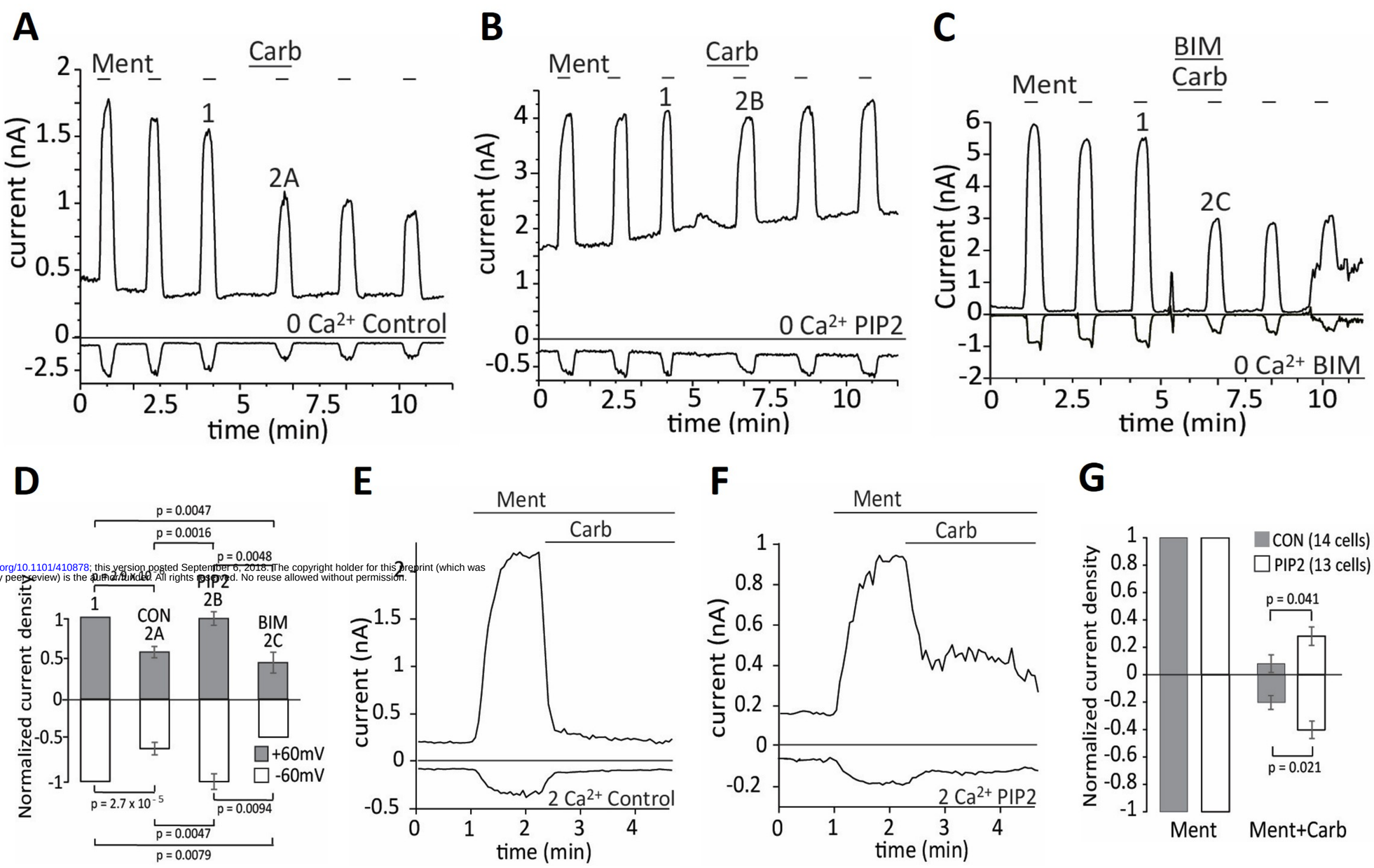

Figure 5

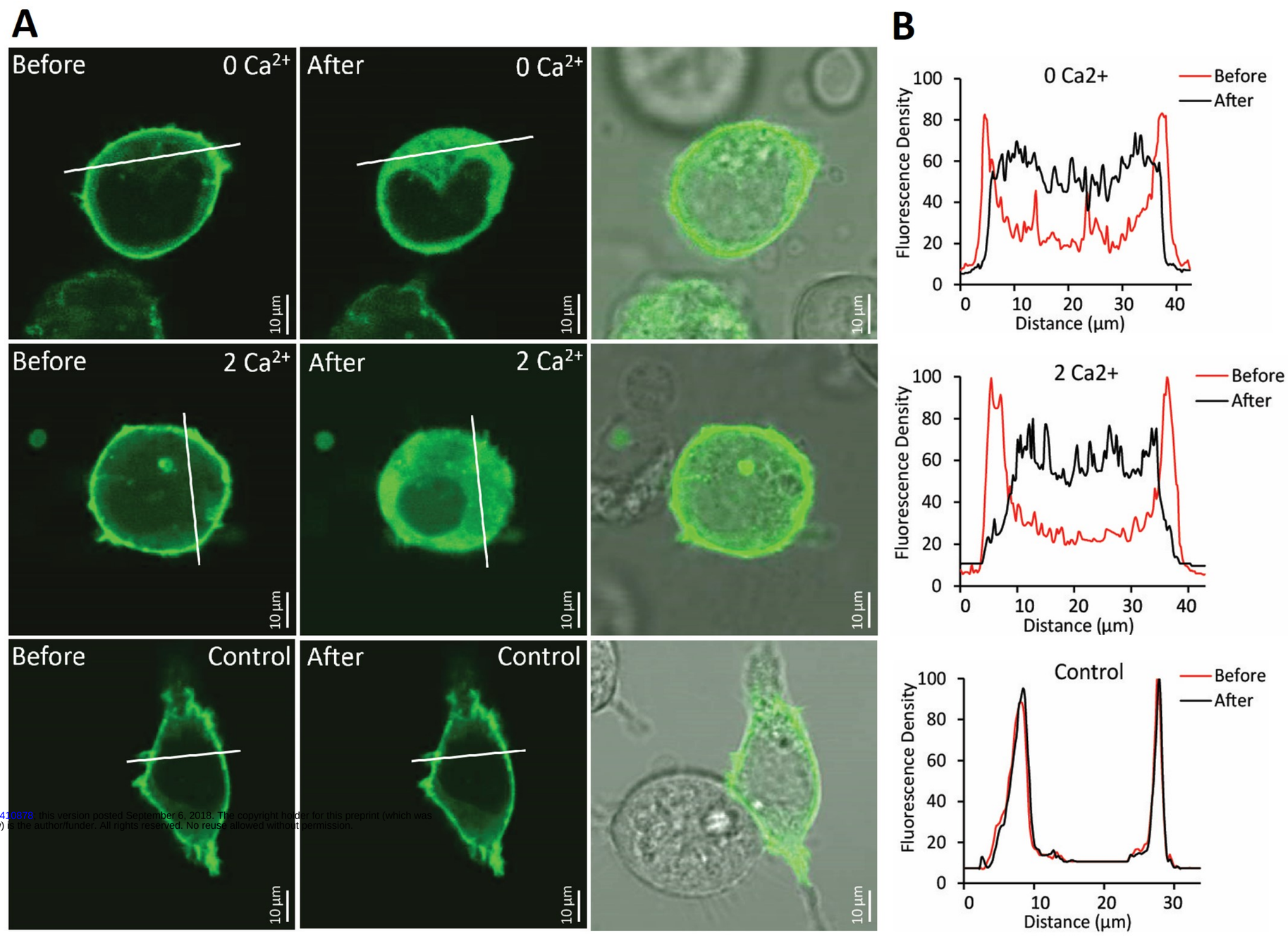

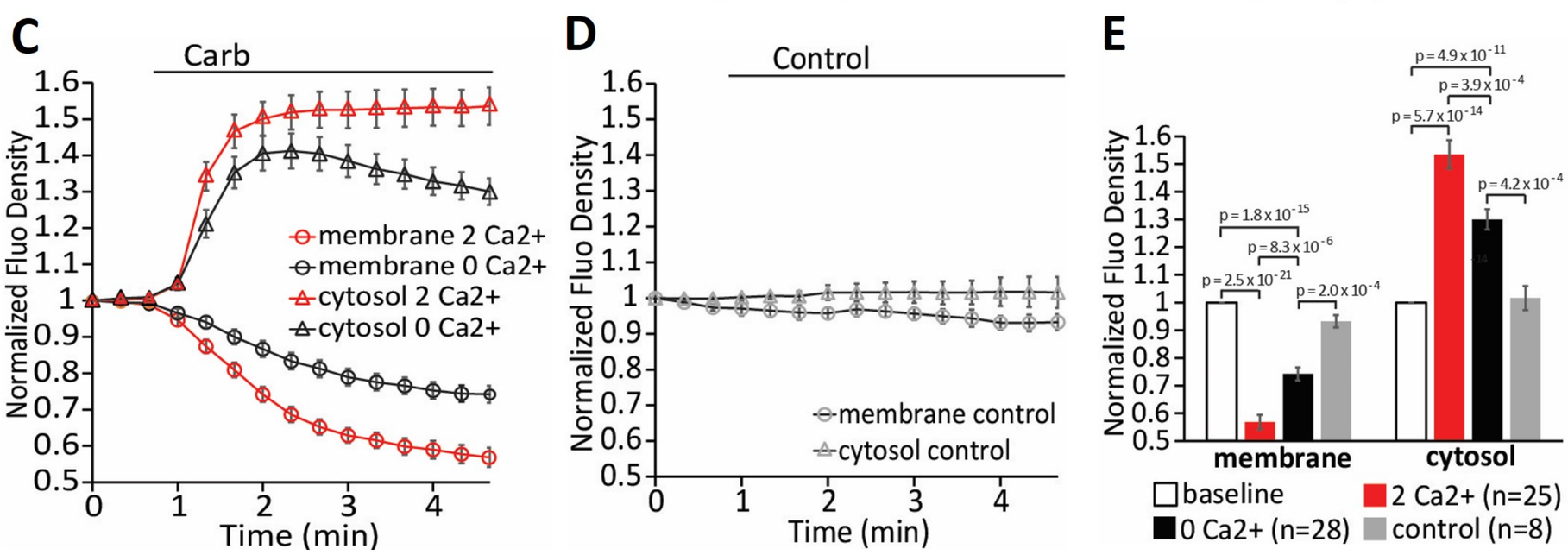

Figure 6

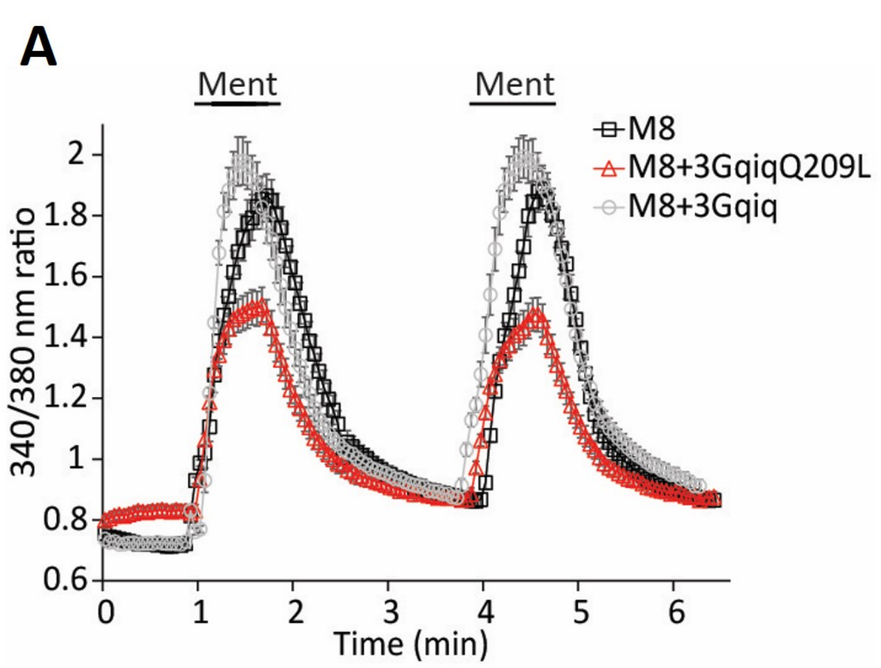

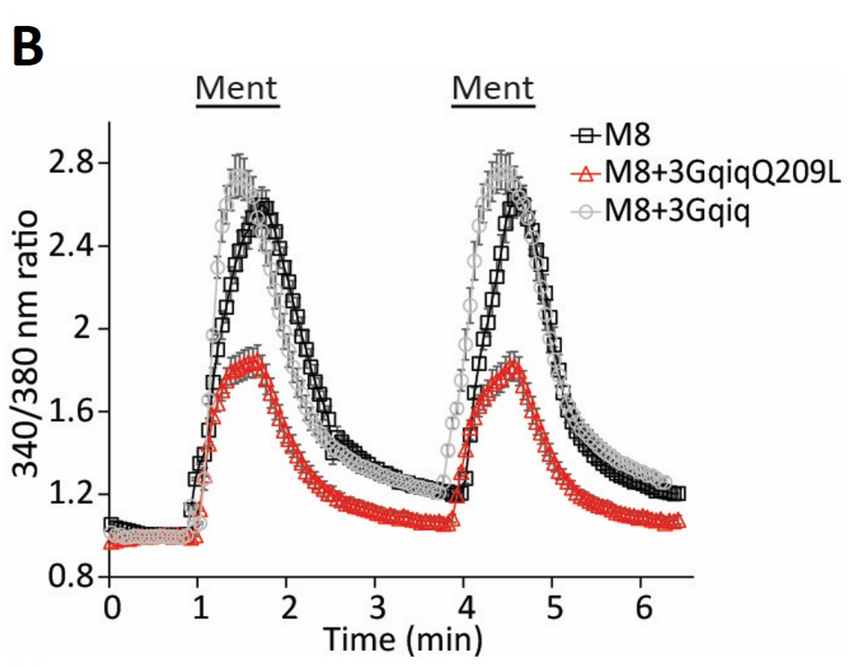

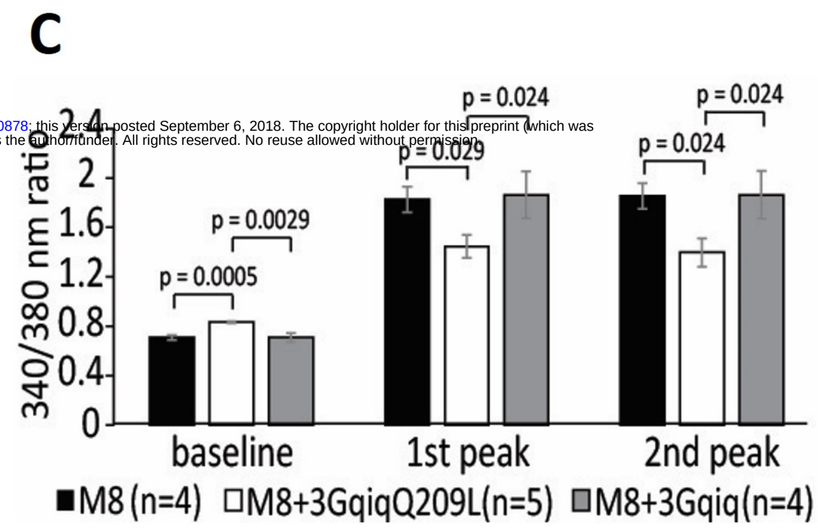

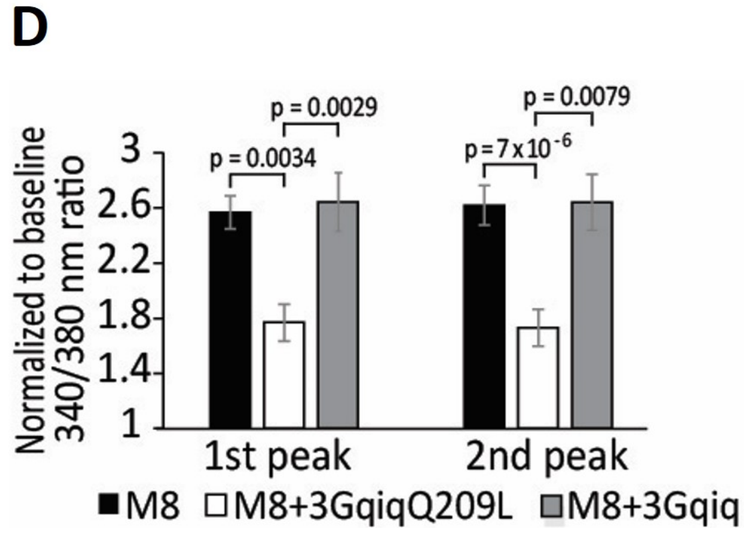

Figure 7